SELECTED QUALITATIVE ASPECTS OF LIDAR POINT CLOUDS: GEOSLAM ZEB-REVO AND FARO FOCUS 3D X130

A. Warchoł [1]*, T. Karaś [2], M. Antoń [3]

[1] Dept. of Geodesy and Geomatics, Faculty of Environmental Engineering, Geomatics and Renewable Energy, Kielce University of Technology, Poland - awarchol@tu.kielce.pl
[2] Faculty of Technical Engineering, State University of Applied Sciences in Jaroslaw - kx.tomasz@gmail.com
[3] Faculty of Technical Engineering, State University of Applied Sciences in Jaroslaw - michal.anton@wp.pl

KEY WORDS: point clouds, BIM, HBIM, terrestrial laser scanning, mobile laser scanning, SLAM, quality.

ABSTRACT:

This paper presents a comparison of LiDAR point clouds acquired using two, different measurement techniques: static TLS (Terrestrial Laser Scanning) performed with a FARO Focus3D X130 laser scanner and a SLAM-based (Simultaneous Localization and Mapping) unit of MLS (Mobile Laser Scanning), namely GeoSLAM ZEB-REVO. After the two point clouds were brought into a single coordinate system, they were compared with each other in terms of internal accuracy and density. The density aspect was visualized using 2D density rasters, and calculated using 3 methods available in CloudCompare software. Thus, one should consider before choosing how to acquire a LiDAR point cloud whether a short measurement time is more important (ZEB-REVO) or whether higher density and measurement accuracy is more important (FARO Focus3D X130). In BIM/HBIM modeling applications, logic dictates that the TLS solution should be chosen, despite the longer data acquisition and processing time, but with a cloud with far better quality parameters that allow objects on the point cloud to be recognized. In a situation where the TLS point cloud is 20 times more dense, it allows to model objects at the appropriate level of geometric detail.

1. INTRODUCTION

LiDAR point clouds are a very popular set of geospatial data that is used in various areas of human activity. Examples of use can be found in many publications:

- environmental mapping and assessment of the state of the natural environment Chiappini et al. (2022), Wężyk et al. (2019), Balestra et al. (2022), Przewoźna et al. (2021), Kovanič e. al. (2020b), Apollo et al. (2023), Krok et al. (2020);
- documentation of cultural heritage Herrero-Tejedor et al. (2023), Warchoł and Łącznar (2022), Sobura et al. (2023), Gawronek et al. (2017), Liu, et al. (2023), Rzonca (2018), Prokop et al. (2021), Gawronek and Noszczyk (2023), Bieda et al. (2021), Skrzypczak et al. (2023);
- inventories of building objects to create 3D BIM (Building Information Modeling) models Skrzypczak et al. (2022), Colucci et al. (2021);

In addition to the issues of point cloud acquisition and application, further life stages of these datasets are also studied, at the level of:

- data processing Błaszczak-Bąk et al. (2022), Kovanič et al. (2020a), Szulwic and Tysiąc (2018);
- integration Bakuła et al. (2022), Tysiąc et al. (2023); or
- publication Quattrini et al. (2017), Malinverni et al. (2019), Pierdicca et al. (2022).

They are also used in engineering works: - architectural inventories - creating as-built BIM (Building Information Modeling) models To ensure the expected accuracy of mapping reality, there is a need to make LiDAR point clouds of a certain quality. According to ISO 19157, this quality consists 6 issues: completeness, logical consistency, position accuracy, thematic accuracy, time accuracy and application. The main problem is the answer for the question: fast measurement or good quality?

Warchoł (2019) proposed to add an additional density parameter that directly affects the possibility or not of mapping certain objects from the point cloud. The best solution is a dense, accurate and even cloud. The uniformity parameter was introduced, for example, in work of Kurczyński and Bakuła (2013), but it was the ALS (Airborne Laser Scanning) perspective, in which it is much easier to maintain the uniformity of data density. In TLS (Terrestrial Laser Scanning) or MLS (Mobile Laser Scanning) data it is definitely more difficult.

Dense and accurate datasets are most easily achieved through the use of TLS. Unfortunately, their downside is usually the length of time spent in the field and the registration of all scan stations to the one, homogeneous project.
The answer to the above problems may be MLS in the form of SLAM (Simultaneous Localization and Mapping) solutions. Some examples could be found in publication of Keitaanniemi et al. (2020) and Wajs et al. (2018). A comprehensive and content-filled literature review about MLS can be found in work di Stefano et. al. (2021). However, the definite minuses of this solution are the density of the obtained point cloud and the accuracy of the measurements.

* Corresponding author

https://doi.org/10.5194/isprs-archives-XLVIII-1-W3-2023-205-2023 | © Author(s) 2023. CC BY 4.0 License.

From the point of view of using a point cloud, its density is one of the key parameters, as it determines whether or not it can be used for a specific purpose. A detailed analysis from the point of view of creating BIM/HBIM models is presented in Warchoł and Lęcznar's (2022) paper. From this work also comes a fig. 1 and 2.

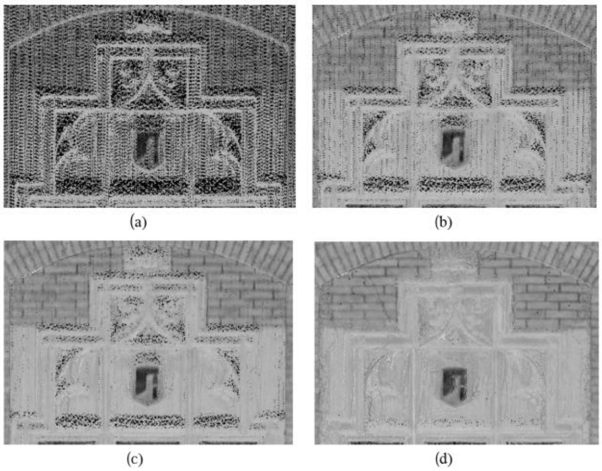

Figure 1. Point cloud of the details above the window at different resolutions acquired with the FARO Focus3D X130 scanner: a) F_1/8, b) F_1/5, c) F_1/4, d) F_1/2

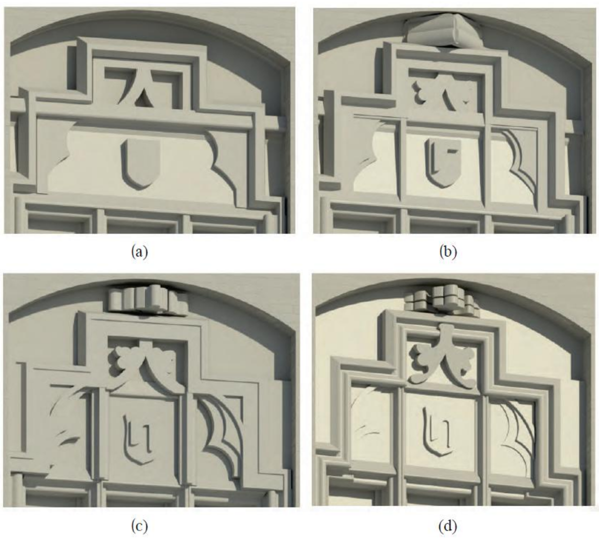

Figure 2. Window details model developed from point clouds with different FARO resolution: (a) F_1/8, (b) F_1/5, (c) F_1/4, (d) F_1/2

At low resolutions (fig. 1a), some elements are not visible on the cloud, and thus cannot be modeled properly or at all.

2. MATERIAL AND METHODS

2.1 Data sets and data aquisitions

This paper presents the parameters characterizing two sets of LiDAR data obtained for the same objects - elevations of 3 buildings ("Biblioteka" - Library, "Instytut Inżynierii Technicznej" - IIT and "Rektorat" - Rector's Office). The exterior dimensions of the buildings were approximately: the "Biblioteka" 62 x 22.5 m and 10.8 m high, "IIT" 55.5 x 22 m and 8.2 m high and "Rektorat" 55.6x 21.3 m and 10.1m high.

The first set is a point cloud from the terrestrial LiDAR laser scanner - FARO Focus 3D X130, while the second was obtained using the GeoSLAM ZEB-REVO scanner - fig. 3.

Figure 3. Used equipment: GeoSLAM ZEB-REVO (left) and FARO Focus 3D X130 (right).

The point clouds from the FARO scanner were acquired in May 2019, from 40 scan station (fig. 4) with nominal resolution of the clouds 7.6 mm at 10 m distance. Project was registered in the FARO SCENE 7.1.0.12 software using cloud-to-cloud method. The average error of registration of 40 scan stations was 23.1 mm, while the maximum was 38.6 mm. Range from 0.6 to 130 m with nominal range error ± 2 mm. Ranging noise defined by the producer is 0.3-0.4 mm at 10m and 0.3-0.5 mm at 25m distance. The lower values correspond to surfaces with 90% reflectivity, while the upper values correspond to surfaces with 10% reflectivity (Faro, 2014).

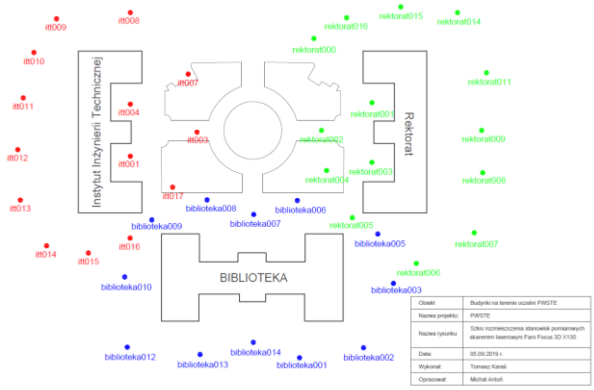

Figure 4. Location of the FARO Focus 3D X130 scan position.

The final point cloud contained over 480 million points, to which, in addition to the intensity, RGB values were also assigned from the images acquired by the scanner. Additionally the FARO data set was cleaned manually and cut in Autodesk ReCap software. Post processed point cloud could be seen on figure 5.

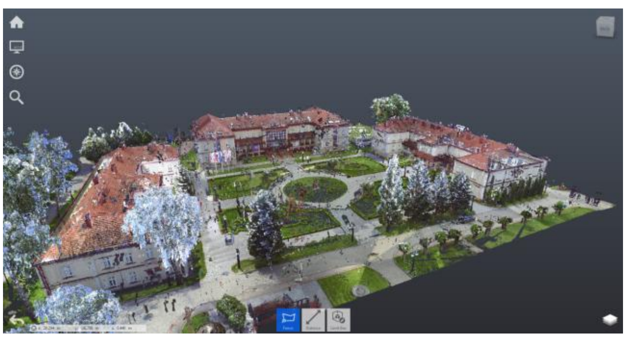

Figure 5. FARO Focus 3D X130 point cloud coloured by RGB values.

The whole project remained in the local coordinate system without georeferencing to the national coordinates system. When comparing the density and internal accuracy of point clouds, their location in space is not crucial. Location of FARO scanner stations on fig. 4 was shown.

The project acquired by the ZEB-REVO scanner, operating as SLAM (Simultaneous Localization And Mapping) in one measurement lasting about 18 minutes and contains almost 16 million points. The whole ZEB-REVO data sets with the shape of the trajectory (green) is shown on fig. 6 and was acquired in June 2017. Area of interest is marked red, contains almost 15 million points and the measurement took 16.5 minutes. Maximum range of the ZEB-REVO is up to 30m in optimal conditions. Typical maximum range is 15-20 m. Scan range noise ±30mm (GeoSLAM, 2017).

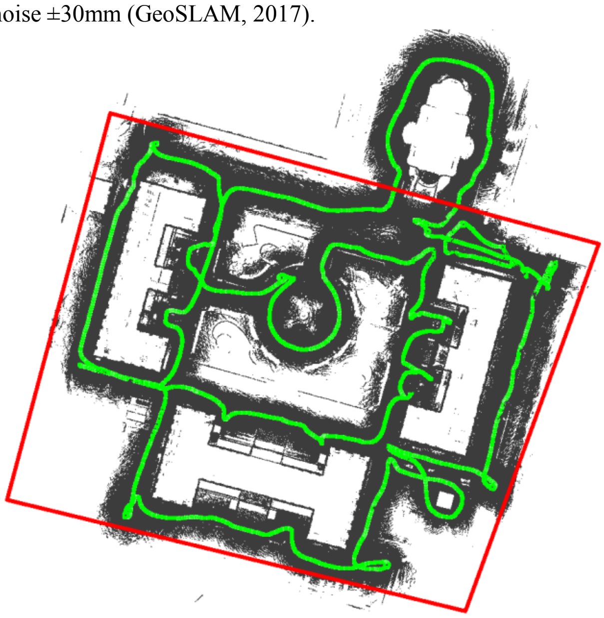

Figure 6. Shape of the GeoSLAM ZEB-REVO trajectory (green) with the acquired point cloud in background. Area of interest marked in red.

Due to the characteristics of the ZEB-REVO measuring device and the relatively short range (up to 30m), the trajectory was in close proximity to building walls. The geometry of such a solution results in a lack of roof data, as can be seen on fig. 6 and fig. 8.

Due to the fact that each of the clouds (ZEB and FARO) was obtained in a local coordinate system, there was a need to shift them to one system. For this purpose, ZEB point clouds were transformed into FARO using the Align Cloud tool in CloudCompare software, separately for each building based on 4 tie points, obtaining RMS values of 3.3 cm for object "Biblioteka ", 4.4 cm for "IIT" and 4.7 cm for "Rektorat", respectively.
The point clouds in the same, local coordinates system imported to the CloudCompare software, colour by intensity could be seen on figure 7 for FARO and figure 8 for ZEB-REVO.

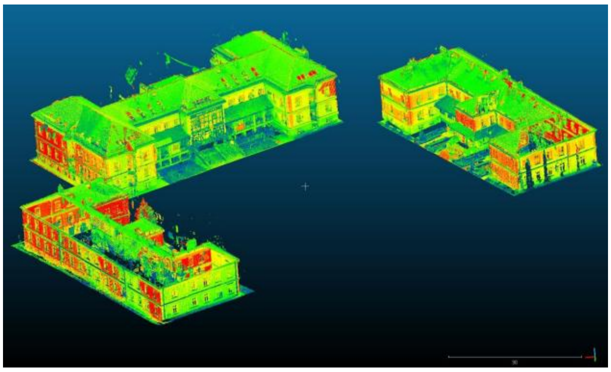

Figure 7. FARO Focus 3D X130 point cloud coloured by intensity values, imported to CloudCompare after shifted to one coordinates system.

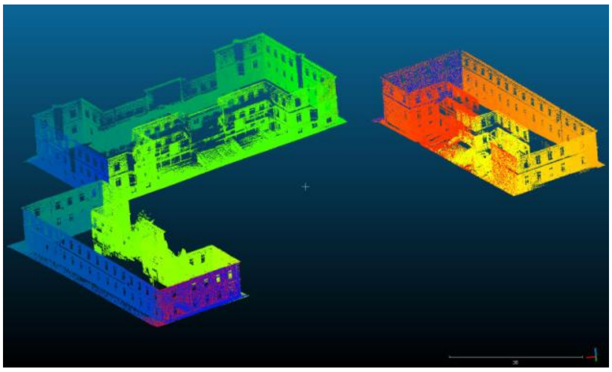

Figure 8. ZEB-REVO point cloud coloured by trajectory, imported to CloudCompare after shifted to one coordinates system.

2.2 Data sets evaluation

The clouds were compared with each other in terms of:
1. geometrical accuracy of the presented objects - based on the differences in the coordinates of the selected 30 points after georeferencing, and
2. point cloud density. The check was made in the CloudCompare software, using the Cloud Density tool in the options: number of neighbours, surface density and volume density.
The methods of calculating the density, listed above are consistent with the considerations contained in publication Warchoł (2015).

3. RESULTS

As presented in Chapter 3, TLS and MLS point clouds were compared in 2 aspects: geometrical accuracy and point cloud density.
First aspect (geometrical accuracy) was checked on 30 points (by 10 on every building) after georeferency. Summary results are presented in Table 1.

	ΔX [m]	ΔY [m]	ΔZ [m]	Dist 2D [m]	Dist 3D[m]
Rektorat					
Min.	-0,022	-0,079	-0,069	0,010	0,043
Max	0,073	0,056	0,040	0,082	0,093
Mean	0,027	0,006	-0,009	0,053	0,067
Std. dev.	0,033	0,043	0,039	0,025	0,021

Biblioteka					
Min.	-0,059	-0,062	-0,063	0,021	0,023
Max	0,056	0,057	0,048	0,082	0,091
Mean	-0,009	0,008	-0,014	0,052	0,059
Std. dev.	0,040	0,041	0,029	0,020	0,024
IIT					
Min.	-0,075	-0,049	-0,072	0,018	0,038
Max	0,066	0,046	-0,001	0,082	0,099
Mean	-0,012	-0,005	-0,037	0,050	0,068
Std. dev.	0,046	0,031	0,029	0,022	0,019

Table 1. Characteristics of differences on each coordinates (FARO minus ZEB) and on the distance (in 2D and in 3D)

Second aspect (point cloud density) is showing in the most simplified form on the fig. 9 and fig. 10. Additionally was checked by 3 methods implemented in CloudCompare software: number of neighbours, surface density and volume density - all in 3D space.

Figure 9 and figure 10 were prepared to show general difference in density of the point clouds from both units. Not for showing precise value of density in every fragment of the area of interest, but to show a scale of difference. Keep in mind that in this approach points from 3D space are counted into 2D GRID. Size of the pixel of the density raster is 0.1m. White area corresponds with 0-19 point in pixel, yellow 20-1999 points, orange 2000-19 999 points and red over 20 000 points. In this approach average of density for FARO point cloud is 23 993 points per m^2, whereas for the ZEB "only" 806 points per m^2.

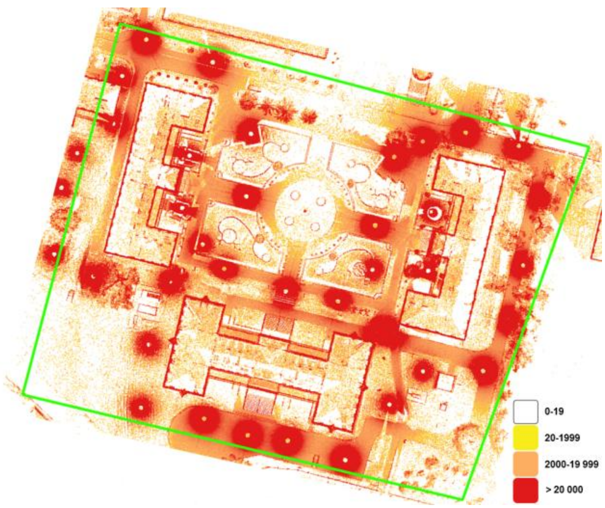

Figure 9. FARO Focus 3D X130 point cloud density, as a raster of density with 0.1m GRID.

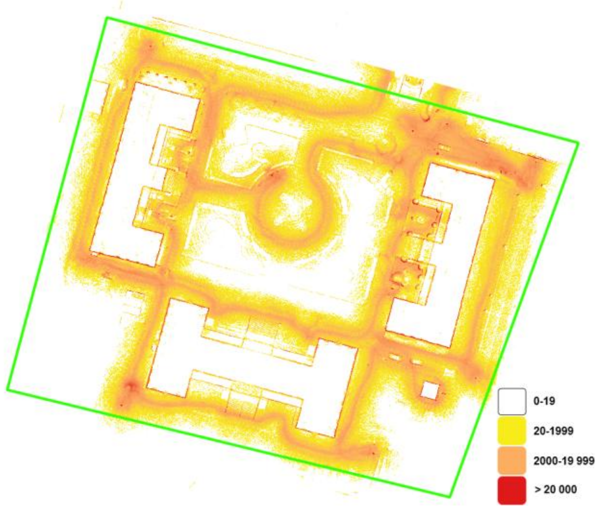

Figure 10. ZEB-REVO point cloud density, as a raster of density with 0.1m GRID.

First of 3D method - "number of neighbours" is counting the number of neighbours for each point in the cloud inside setting radius (r) - in this case 2 cm (CloudCompare). Histograms of this method for FARO data set is showing on figure 11, while for ZEB-REVO on figure 12.

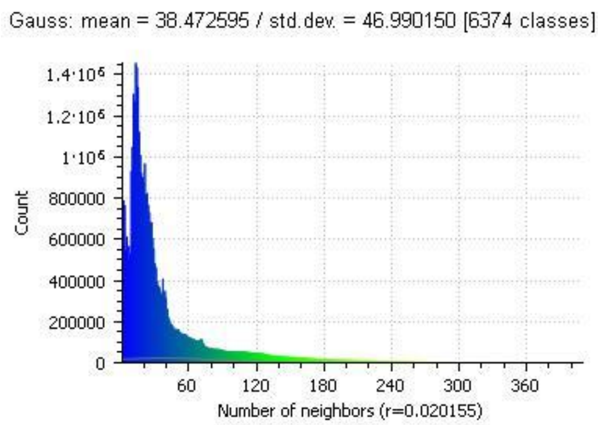

Figure 11. Histogram of "number of neighbours" method for FARO Focus 3D X130 point cloud.

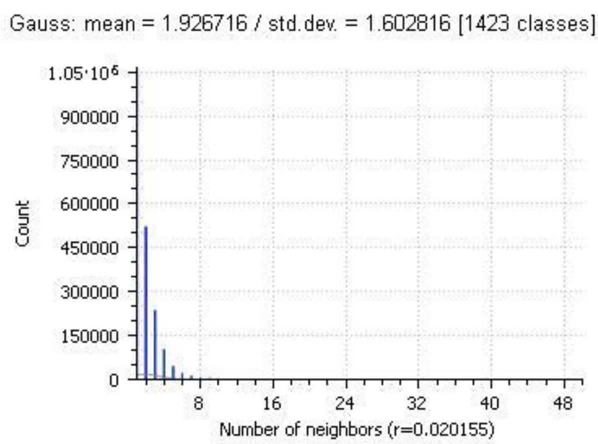

Figure 12. Histogram of "number of neighbours" method for ZEB-REVO point cloud.

Second of 3D method - "surface density" is counting the number of neighbours divided by the neighbourhood surface with 2 cm radius (r) - details on (CloudCompare). Histograms of this method for FARO data set is showing on figure 13, while for ZEB-REVO on figure 14.

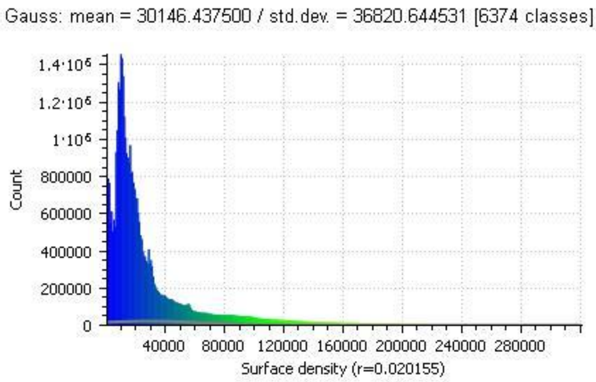

Figure 13. Histogram of "surface density" method for FARO Focus 3D X130 point cloud.

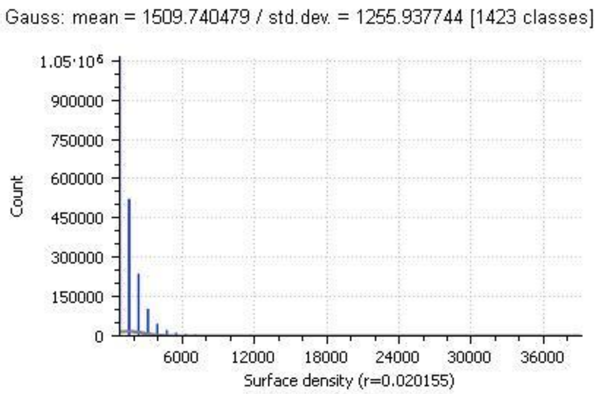

Figure 14. Histogram of "surface density" method for ZEB-REVO point cloud.

Third of 3D method - "volume density" is counting the number of neighbours divided by the neighbourhood volume with 2 cm radius (r) - details on (CloudCompare). Histograms of this method for FARO data set is showing on figure 15, while for ZEB-REVO on figure 16.

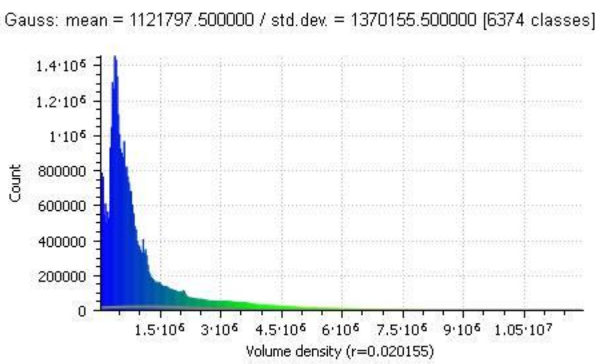

Figure 15. Histogram of "volume density" method for FARO Focus 3D X130 point cloud.

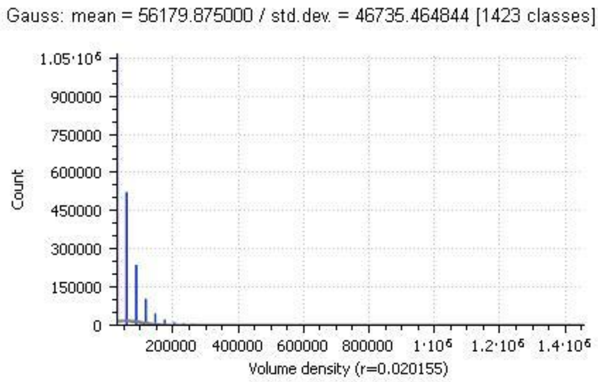

Figure 16. Histogram of "volume density" method for ZEB-REVO point cloud.

As can be seen in fig. 9 and 10 and in histograms 11-16, the differences in point cloud density are significant. Regardless of how the density is counted, the FARO data is at least 20 times denser than ZEB-REVO. This also translates into the visual effect presented on fig. 17-20.

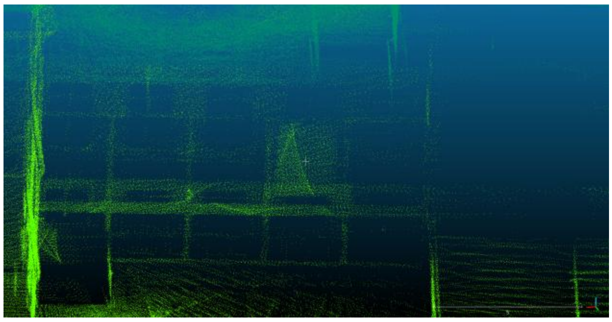

Figure 17. Point cloud of the "Biblioteka" object acquired by the GeoSLAM ZEB-REVO colored by trajectory.

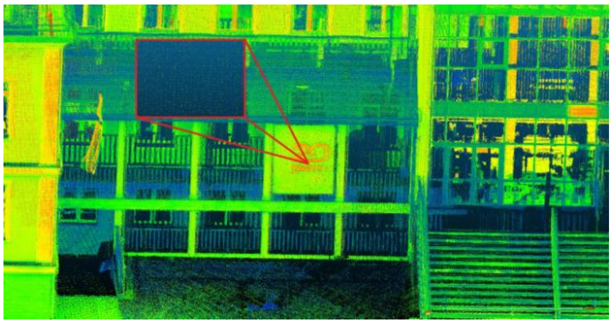

Figure 18. Point cloud of the "Biblioteka" object acquired by the FARO Focus 3D X130 colored by the intensity.

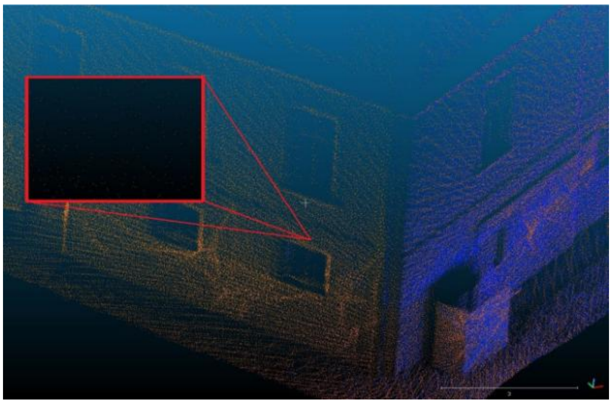

Figure 19. Point cloud of the "IIT" object acquired by the GeoSLAM ZEB-REVO colored by trajectory.

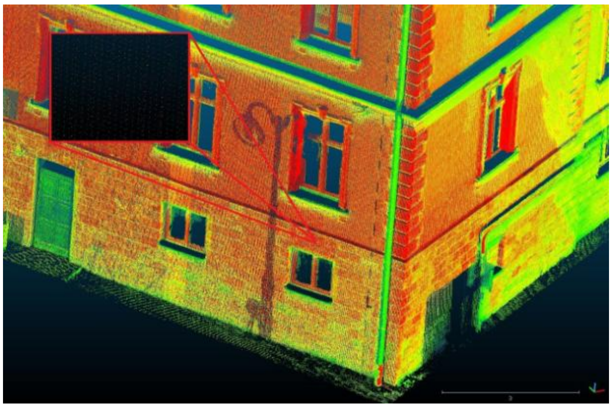

Figure 20. Point cloud of the "IIT" object acquired by the FARO Focus 3D X130 colored by the intensity.

4. CONCLUSIONS

The first issue, geometrical accuracy, was checked on 30 pairs of points, 10 pairs of points for each building. The differences for each coordinate take on both positive and negative values, stacking up as to values in similar ranges. Thus, no clear systematic errors can be seen at any of the coordinates. The values of the average 3D distances between corresponding points on both clouds are higher than the RMS of matching clouds between them. The differences between the 3D distances from Table 1 and the RMS, indicate an additional error component of 2cm for the "Rektorat" object, 2.6cm for the "Biblioteka" object and 2.4cm for the "IIT" object. Thus, these are the values contributed to the final point cloud by the ZEB-REVO measurement unit and/or the MLS point cloud alignment.

In the second aspect controlled, i.e., the density of the final point clouds, the large standard deviation indicates large differences in local point cloud density, i.e., there are areas in which the density is markedly different. This is evident, for example, in figures 9 and 10 where one can see a large number of white pixels, i.e., with densities of 0-19 pts/m2 and areas with red pixels with point counts of more than 20,000 pts/m2 near scanning equipment.

Thus, one should consider before choosing how to acquire a LiDAR point cloud whether a short measurement time is more important to the recipient, as in ZEB-REVO, or whether higher density and measurement accuracy is more important, as in FARO Focus3D X130. In BIM/HBIM modeling applications, logic dictates that the TLS solution should be chosen, despite the longer data acquisition and processing time, but with a cloud with far better quality parameters that allow objects on the point cloud to be recognized (figures 17-20). In a situation where the TLS point cloud is 20 times more dense, it allows to model objects at the appropriate level of geometric detail.

ACKNOWLEDGEMENTS

The point cloud acquired with the ZEB-REVO laser scanner was made available by Przedsiębiorstwo Usług Geodezyjnych - Projektowych "Geomiar" Sp. z o. o. from Jaroslaw for scientific purposes.

REFERENCES

Apollo, M., Jakubiak, M., Nistor, S., Lewińska, P., Krawczyk A., Borowski, Ł., Specht, M., Krzykowska-Piotrowska, K., Marchel, Ł., Pęska-Siwik, A., Kardoš, M., Maciuk, K., 2023. Geodata in science - a review of selected scientific fields, Acta Scientiarum Polonorum Formatio Circumiectus, vol. 22, nr 2, 2023, s. 17-40, DOI:10.15576/ASP.FC/2023.22.2.02

Bakuła, K., Lejzerowicz, A., Pilarska-Mazurek, M., Ostrowski, W., Górka, J., Biernat, P., Czernic, P., Załęgowski, K., Kleszczewska, K., Wężka, K., Gąsiewski, M., Dmowski, H., Styś, N., 2022. "SENSOR INTEGRATION AND APPLICATION OF LOW-SIZED MOBILE MAPPING PLATFORM EQUIPPED WITH LIDAR, GPR AND PHOTOGRAMMETRIC SENSORS." In International Archives of the Photogrammetry, Remote Sensing and Spatial Information Sciences - ISPRS Archives, 43:167–72. https://doi.org/10.5194/isprs-archives-XLIII-B1-2022-167-2022.

Balestra, M., Chiappini, S., Vitali, A., Tonelli, E., Malandra, F., Galli, A., Urbinati, C., Malinverni, E.S., Pierdicca, R., 2022. "INTEGRATION OF GEOMATIC TECHNIQUES FOR THE 3D REPRESENTATION AND MONITORING OF A VETERAN CHESTNUT TREE." In International Archives of the Photogrammetry, Remote Sensing and Spatial Information Sciences - ISPRS Archives. Vol. 43. https://doi.org/10.5194/isprs-archives-XLIII-B3-2022-833-2022.

Bieda, A., Balawejder, M., Warchoł, A., Bydłosz, J., Kolodiy, P. and Pukanská, K., 2021. Use of 3D technology in underground tourism: example of Rzeszow (Poland) and Lviv (Ukraine). Acta Montanistica Slovaca. Volume 26 (2) 205-221, DOI: 10.46544/AMS.v26i2.03

Błaszczak-Bąk, W., Suchocki, C., Mrówczyńska, M., 2022. "Optimization of Point Clouds for 3D Bas-Relief Modeling." Automation in Construction 140. https://doi.org/10.1016/j.autcon.2022.104352.

Chiappini, S., Pierdicca, R., Malandra, F., Tonelli, E., Malinverni, E.S., Urbinati, C., Vitali, A., 2022. "Comparing Mobile Laser Scanner and Manual Measurements for Dendrometric Variables Estimation in a Black Pine (Pinus Nigra Arn.) Plantation." Computers and Electronics in Agriculture 198. https://doi.org/10.1016/j.compag.2022.107069.

Colucci, E.; Xing, X.; Kokla, M.; Mostafavi, M.A.; Noardo, F.; Spanò, A., 2021. Ontology-Based Semantic Conceptualisation of Historical Built Heritage to Generate Parametric Structured

Models from Point Clouds. *Appl. Sci.* 2021, *11*, 2813. https://doi.org/10.3390/app11062813

CloudCompare, - https://www.cloudcompare.org/doc/wiki/index.php/Density access 8.09.2023

Di Stefano, F., Chiappini, S., Gorreja, A., Balestra M., Pierdicca, R., 2021. Mobile 3D scan LiDAR: a literature review, Geomatics, Natural Hazards and Risk, 12:1, 2387-2429, DOI: 10.1080/19475705.2021.1964617

Gawronek, P., Makuch, M., Mitka, B., Bożek, P., Klapa, P., 2017. "3D SCANNING OF THE HISTORICAL UNDERGROUND OF BENEDICTINE ABBEY IN TYNIEC (POLAND)." In International Multidisciplinary Scientific GeoConference : SGEM - Section Geodesy and Mine Surveying. https://doi.org/10.5593/sgem2017/22.

Gawronek, P., Noszczyk, T., 2023. Does more mean better? Remote-sensing data for monitoring sustainable redevelopment of a historical granary in Mydlniki, Kraków. Herit Sci 11, 23 (2023). https://doi.org/10.1186/s40494-023-00864-0

Herrero-Tejedor, T.R., Maté-González, M.A., Pérez-Martín, E., López-Cuervo, S., de Herrera, J.L., Sánchez-Aparicio, L.J., Llauradó, P.V., 2023. "Documentation and Virtualisation of Vernacular Cultural Heritage: The Case of Underground Wine Cellars in Atauta (Soria)." Heritage 6 (7): 5130–50. https://doi.org/10.3390/heritage6070273.

Keitaanniemi, A., Kukko, A., Virtanen, J-P., Vaaja, M., 2020. MEASUREMENT STRATEGIES FOR STREET-LEVEL SLAM LASER SCANNING OF URBAN ENVIRONMENTS. The Photogrammetric Journal of Finland, Vol. 27, No. 1, Doi:10.17690/020271.1

Kovanič, Ľ.; Blistan, P.; Urban, R.; Štroner, M.; Pukanská, K.; Bartoš, K.; Palková, J., 2020. Analytical Determination of Geometric Parameters of the Rotary Kiln by Novel Approach of TLS Point Cloud Segmentation. *Appl. Sci.* 2020, *10*, 7652. https://doi.org/10.3390/app10217652

Kovanič, Ľ.; Blistan, P.; Urban, R.; Štroner, M.; Blišťanová, M.; Bartoš, K.; Pukanská, K. 2020. Analysis of the Suitability of High-Resolution DEM Obtained Using ALS and UAS (SfM) for the Identification of Changes and Monitoring the Development of Selected Geohazards in the Alpine Environment—A Case Study in High Tatras, Slovakia. *Remote Sens.* 2020, *12*, 3901. https://doi.org/10.3390/rs12233901

Krok, G., Kraszewski, B., Stereńczak, K. 2020. Application of terrestrial laser scanning in forest inventory – an overview of selected issues. Leśne Prace Badawcze / Forest Research Papers, 81(4), 175-194. doi:10.2478/frp-2020-0021.

Kurczyński, Z., Bakuła, K., 2013. Generation of countrywide reference Digital Terrain Model from Airborne Laser Scannig in ISOK project, Archives of Photogrammetry, Cartography and Remote Sensing, APCRS special issue – Warszawa, 59-68. http://ptfit.sgp.geodezja.org.pl/wydawnictwa/monografia/09-Kurczynski.pdf

Liu, J.; Willkens, D.; Gentry, R. 2023. A Conceptual Framework for Integrating Terrestrial Laser Scanning (TLS) into the Historic American Buildings Survey (HABS). *Architecture* 2023, *3*, 505-527. https://doi.org/10.3390/architecture3030028

Malinverni, E. S., Chiappini, S., Pierdicca, R., 2019. "A Geodatabase for Multisource Data Management Applied to Cultural Heritage: The Case Study of Villa Buonaccorsi's Historical Garden." In ISPRS Annals of the Photogrammetry, Remote Sensing and Spatial Information Sciences. Vol. 42. https://doi.org/10.5194/isprs-Archives-XLII-2-W11-771-2019.

Pierdicca, R., Mulliri, M., Lucesoli, M., Piccinini, F., Malinverni, E.S., 2022. "Geomatics Meets XR: A Brief Overview of the Synergy Between Geospatial Data and Augmented Visualization." In Lecture Notes in Computer Science (Including Subseries Lecture Notes in Artificial Intelligence and Lecture Notes in Bioinformatics). Vol. 13446 LNCS. https://doi.org/10.1007/978-3-031-15553-6_17.

Prokop, A., Nazarko, P. and Ziemiański, L. 2021. Digitalization of historic buildings using modern technologies and tools, *Budownictwo i Architektura*, 20(2), pp. 083-094. doi: 10.35784/bud-arch.2444.

Przewoźna, P.; Hawryło, P.; Zięba-Kulawik, K.; Inglot, A.; Mączka, K.; Wężyk, P.; Matczak, P., 2021. Use of Bi-Temporal ALS Point Clouds for Tree Removal Detection on Private Property in Racibórz, Poland. *Remote Sens.* 2021, *13*, 767. https://doi.org/10.3390/rs13040767

Quattrini, R., Pierdicca, R., Morbidoni, Ch., Malinverni, E.S., 2017. "CONSERVATION-ORIENTED HBIM. THE BIMEXPLORER WEB TOOL. WG HBIM for Management and Maintenance." The International Archives of the Photogrammetry, Remote Sensing and Spatial Information Sciences XLII (5): 275–83. https://doi.org/10.5194/isprs-archives-XLII-5-W1-275-2017.

Rzonca, A., 2018. Digital documentation of heritage objects on non-developable surfaces. 2018 Baltic Geodetic Congress. DOI: 10.1109/BGC-Geomatics.2018.00036

Skrzypczak, I., Oleniacz, G., Leśniak, A., Zima, K., Mrówczyńska, M., Kazak, J. K.,. 2022. "Scan-to-BIM Method in Construction: Assessment of the 3D Buildings Model Accuracy in Terms Inventory Measurements." Building Research and Information 50 (8): 859–880. https://doi.org/10.1080/09613218.2021.2011703.

Skrzypczak, I., Oleniacz, G., Leśniak, A., Mrówczyńska, M., Rymar. M., Oleksy, M., 2023. A practical hybrid approach to the problem of surveying a working historical bell considering innovative measurement methods. Herit Sci 11, 152 (2023). https://doi.org/10.1186/s40494-023-01007-1

Sobura, S., Bacharz, K., Granek, G., 2023. "ANALYSIS OF TWO-OPTION INTEGRATION OF UNMANNED AERIAL VEHICLE AND TERRESTRIAL LASER SCANNING DATA FOR HISTORICAL ARCHITECTURE INVENTORY." Geodesy and Cartography 49 (2): 76–87. https://doi.org/10.3846/gac.2023.16990.

Szulwic, J., Tysiąc, P., 2018. MOBILE LASER SCANNING CALIBRATION ON A MARINE PLATFORM. POLISH MARITIME RESEARCH Special Issue 2018 S1 (97) 2018 Vol. 25; pp. 159-165 DOI: 10.2478/pomr-2018-0037

Tysiac, P., Sieńska, A., Tarnowska, M., Kedziorski, P., Jagoda, M., 2023. Combination of terrestrial laser scanning and UAV photogrammetry for 3D modelling and degradation assessment of heritage building based on a lighting analysis: case study—St. Adalbert Church in Gdansk, Poland. Herit Sci 11, 53 (2023). https://doi.org/10.1186/s40494-023-00897-5

Wajs, J., Kasza, D., Zagożdżon, PP., Zagożdżon, KD., 2018. 3D modeling of underground objects with the use of SLAM technology on the example of historical mine in Ciechanowice (Ołowiane Range, The Sudetes). E3S Web of Conferences 29, 00024 doi.org/10.1051/e3sconf/20182900024

Warchoł, A., 2015. Density of point clouds in mobile laser scanning. Archives of Photogrammetry, Cartography and Remote Sensing, vol. 27, 149-161 DOI: 10.14681/afkit.2015.011

Warchoł, A., 2019. The concept of LIDAR data quality assessment in the context of BIM modeling, ISPRS - Int. Arch. Photogramm. Remote Sens. Spatial Inf. Sci. XLII-1/W2, 61–66, http://dx.doi.org/10.5194/isprs-archives-XLII-1-W2- 61-2019

Warchoł, A., Lęcznar J., 2022. "Density of Ground-based LiDAR Point Clouds in the Context of BIM Modeling." In Acquiring Geodetic Data for the Needs of Spatial Management of the Świętokrzyskie Region, edited by Bogdan Wolski and Agnieszka Cienciała, 77-99. Kielce

Wężyk, P., Hawryło, P., Szostak M., Zięba-Kulawik, K., Winczek, M., Siedlarczyk, E., Kurzawiński, A., Rydzyk, J., Kmiecik, J., Gilewski, W., Szparadowska, M., Warchoł, A., Turowska, A., 2019. Using LiDAR Point Clouds in Determination of the Scots Pine Stands Spatial Structure Meaning in the Conservation of Lichen Communities in 'Bory Tucholskie' National Park. Archives of Photogrammetry, Cartography and Remote Sensing 31 (1): 85–103. https://doi.org/10.2478/apcrs-2019-0007.

www.faro.com - Faro Focus 3D X130 TechSheet ver. 2014

www.geoslam.com - GeoSLAM ZEB-REVO User Manual v3.0.0 ver. 2017